Received: 24 March 2021 | Revised: 28 September 2021 | Accepted: 1 October 2021

DOI: 10.1002/rra.3878

RESEARCH ARTICLE

WILEY

Bankfull shear velocity predicts embeddedness and silt cover in gravel streambeds

Jonathan A. Czuba[1,2] | Mallory Hirschler[3] | Elizabeth A. Pratt[1] | Amy Villamagna[3] | Paul L. Angermeier[2,4]

[1]Department of Biological Systems Engineering, Virginia Tech, Blacksburg, Virginia, USA

[2]The Global Change Center, Virginia Tech, Blacksburg, Virginia, USA

[3]Department of Environmental Science and Policy, Plymouth State University, Plymouth, New Hampshire, USA

[4]U.S. Geological Survey, Virginia Cooperative Fish and Wildlife Research Unit, Department of Fish and Wildlife Conservation, Virginia Tech, Blacksburg, Virginia, USA

Correspondence
Jonathan A. Czuba, Department of Biological Systems Engineering, Virginia Tech, Blacksburg, Virginia, USA.
Email: jczuba@vt.edu

Funding information
National Fish and Wildlife Foundation, Grant/Award Number: 8020.18.059147; National Institute of Food and Agriculture, Grant/Award Number: 1017457; Virginia Agricultural Experiment Station, Virginia Polytechnic Institute and State University

Abstract

Excess fine sediment (<2 mm) deposition on gravel streambeds can degrade habitat quality for stream biota. Two measures of fine sediment deposition include embeddedness and silt cover (<62.5 μm). Embeddedness measures fine sediment in interstitial pore spaces, whereas silt cover, primarily deposited during low flows, measures fine sediment draped on the streambed's surface. Here, we demonstrate that a baseline level of embeddedness and a maximum value of silt cover can be predicted from bankfull shear velocity, which can be estimated from river channel and streamflow characteristics, independently of knowing the sediment supply. We derive an equation for bankfull shear velocity that only requires knowing bankfull flow, channel width, and channel slope, which can be readily obtained in the United States from freely available, remotely sensed data. We apply this methodology to data collected at 30 sites in the Piedmont region of Virginia and North Carolina. This work is an important step in developing statistical models of stream ecosystems in which geophysical variables can predict embeddedness and silt cover, which commonly limit biotic assemblages.

KEYWORDS
colmation, fine sediment, gravel-bed river, sediment deposition, sediment infiltration, sediment supply, stream habitat, winnowing

1 | INTRODUCTION

Excess fine sediment is a chronic, widespread, and major cause of impairment in streams across the United States (USEPA, 2020). Fine sediment impairment contributes to the imperilment of many aquatic species (Kemp, Sear, Collins, Naden, & Jones, 2011; Wharton, Mohajeri, & Righetti, 2017; Wood & Armitage, 1997). When fine sediment (<2 mm in diameter) deposits on a streambed, it can move into and accumulate within pore spaces between coarser particles (>2 mm in diameter), such as gravels and cobbles. This process of colmation is synonymous with fine sediment deposition and infiltration, clogging of pore spaces, and infilling, among others (Brunke, 1999; Wharton et al., 2017). Colmation degrades habitat quality for benthic macroinvertebrates and fishes by reducing streambed porosity and oxygenation, interparticle water flow, and surfaces for biological production (see review in Wharton et al., 2017).

Stream ecologists commonly measure embeddedness and silt cover to assess colmation. Embeddedness is a measure of the extent to which coarse particles on the streambed are surrounded by, or embedded into, finer particles. Silt cover is a measure of the amount of the streambed surface covered by very fine sediment (<62.5 μm). Both of these metrics can be assessed visually (e.g., Fitzpatrick et al., 1998). In addition, embeddedness can be quantitatively measured as the vertical distance along a coarse particle that is

surrounded by fine sediment (often indicated by a silt line, stain line, or edge of periphyton growth) relative to the total height of the particle (Fitzpatrick et al., 1998; Sennatt, Salant, Renshaw, & Magilligan, 2006; Sutherland, Culp, & Benoy, 2010). Embeddedness focuses on the amount of fine sediment in the interstitial pore spaces of a coarse streambed measured in the vertical direction, whereas silt cover focuses on the amount of very fine sediment draped on the surface of a streambed. Presently, there are no highly effective methods to estimate or predict embeddedness or silt cover from remotely sensed data.

Prior efforts to predict in-stream embeddedness and silt cover used a suite of watershed and channel metrics in regression models (e.g., Naden et al., 2016; Scott & Villamagna, 2020; Sutherland et al., 2010; Walters, Leigh, Freeman, Freeman, & Pringle, 2003). Overall, these studies found that the amount of fine sediment in the streambed was negatively correlated with stream power (Naden et al., 2016) and channel slope (Relyea, Minshall, & Danehy, 2012; Sutherland et al., 2010; Walters et al., 2003). This suggests that in-channel characteristics that account for the stream's capacity to transport or deposit sediment, in part, determine fine sediment effects on the streambed (Naden et al., 2016).

From a process-based perspective, a sediment particle deposits when its fall velocity exceeds the turbulent shear velocity keeping that particle in suspension (García, 2008; Niño, Lopez, & García, 2003). Lamb and Venditti (2016) showed that a bankfull shear velocity of 0.1 m/s is a critical threshold between a (coarse) gravel bed and a (fine) sand-covered bed. That is, below this critical value (bankfull shear velocity <0.1 m/s), the streambed surface is expected to be completely covered with fine sediment (100% embeddedness). While Lamb and Venditti (2016) focused on the abrupt transition between a gravel and sand bed, we hypothesize that this same framework can be used to predict embeddedness, and perhaps silt cover. Specifically, we expect 100% embeddedness at a bankfull shear velocity of 0.1 m/s, and embeddedness to gradually decrease with increasing shear velocity. These expectations imply that shear velocity could predict differences in embeddedness among intra-stream locations whose local channel geometry and slope contribute to differences in bankfull shear velocity, even under the same sediment supply conditions.

Herein, we demonstrate that embeddedness and silt cover can be predicted from bankfull shear velocity, which can be estimated from stream channel and flow characteristics. We derive four equations for calculating shear velocity depending on what is known at a site. At a minimum, bankfull flow, width, and channel slope, which can be readily obtained in the United States from freely available, remotely sensed data, can be used to estimate bankfull shear velocity. We then test our hypothesis by relating our estimates of bankfull shear velocity to embeddedness and silt cover data we collected at 30 sites in the Piedmont region of Virginia and North Carolina. This work is an important step toward developing predictive ecological models that link geophysical features of streams to in-stream variables such as embeddedness and silt cover, which ultimately influence biotic assemblages.

2 | THEORETICAL DEVELOPMENTS IN COMPUTING SHEAR VELOCITY

For steady, uniform streamflow, water exerts a stress on the streambed known as the bed shear stress τ_b, calculated as

$$\tau_b = \rho g R_h S, \tag{1}$$

where ρ is the density of water, g is the acceleration due to gravity, R_h is the hydraulic radius of the channel (cross-sectional area divided by wetted perimeter), and S is the channel slope. This bed shear stress (force per unit area) can be recast as a shear velocity u_* as

$$u_* = \sqrt{\frac{\tau_b}{\rho}}. \tag{2}$$

Bed shear stress and shear velocity are measures of flow intensity and the ability of flow to move and suspend sediment particles. Substituting Equation (1) into Equation (2), shear velocity can be calculated directly as

$$u_*^x = \sqrt{g R_h S}. \tag{3}$$

The superscript x denotes that this shear velocity was computed with information from a channel cross section. Equation (3) requires knowing the channel slope and the hydraulic radius of the channel R_h, which typically can be calculated only if channel cross-sectional geometry has been measured (g is a constant). Instead, it is often convenient to replace the hydraulic radius with variables that are easier to measure.

Manning's equation relates channel properties to flow discharge Q as

$$Q = \frac{k_n}{n} A R_h^{2/3} S^{1/2}, \tag{4}$$

where k_n is a conversion factor between SI and English units, n is Manning's roughness, and A is the channel cross-sectional area. For wide (width >> depth), rectangular channels, the hydraulic radius R_h can be approximated as the average depth H and the cross-sectional area is the product of channel width B and depth H. Making these simplifications to Equation (4) and rearranging, the average depth H can be calculated as

$$H = \left(\frac{Qn}{k_n B S^{1/2}}\right)^{3/5}. \tag{5}$$

Furthermore, because we have approximated the hydraulic radius R_h as the average depth H, we can substitute Equation (5) into Equation (3) and simplify as

$$u_*^n = g^{1/2} \left(\frac{Qn}{k_n B}\right)^{3/10} S^{7/20}. \tag{6}$$

The superscript n denotes that this shear velocity was computed with a Manning's roughness value. To calculate shear velocity using Equation (6), only flow discharge, channel width, channel slope, and Manning's roughness must be known (g and k_n are constants).

Factors that contribute to roughness in streams include bed sediment particle size, bedforms, bars, channel geometry, vegetation, large wood, and channel planform characteristics (Cowan, 1956). The factors contributing most to roughness vary with stream characteristics. If most roughness is contributed by grain roughness from bed particles, then Manning's roughness can be written (García, 2008) as

$$n = \frac{k_s^{1/6}}{ag^{1/2}}, \tag{7}$$

where k_s is the roughness height and a is the coefficient of the Manning–Strickler form of the logarithmic law for estimating the velocity distribution in the vertical direction. The roughness height can be written (García, 2008) as

$$k_s = \alpha_s D_x, \tag{8}$$

where α_s is a constant and D_x is the xth percentile bed sediment grain size. Substituting Equation (8) into Equation (7), Manning's roughness can be written as

$$n = \frac{\alpha_s^{1/6} D_x^{1/6}}{ag^{1/2}}. \tag{9}$$

However, where grain roughness does not dominate, such as for steep mountain streams where flow resistance is dominated by boulders, large wood, and steps (Lamb, Brun, & Fuller, 2017; Rickenmann & Recking, 2011; Yochum, Bledsoe, David, & Wohl, 2012), this parameterization of roughness (Equation [7]–[9]) does not apply and an alternative formulation should be developed to account for the relevant contributions to roughness. Upon substituting Equation (9) into Equation (6) and rearranging, shear velocity can also be calculated as

$$u_*^D = (\alpha_s D_x)^{1/20} \left(\frac{Q}{ak_n B}\right)^{3/10} (gS)^{7/20}. \tag{10}$$

The superscript D denotes that this shear velocity was computed with a characteristic bed sediment grain size. To calculate shear velocity using Equation (10), only flow discharge, channel width, channel slope, and a characteristic bed sediment grain size must be known (g, k_n, α_s, and a are treated as constants).

The xth percentile bed sediment grain size D_x can be predicted using similar equations as above and assuming that this sediment is mobilized at a specific flow discharge Q_b (Snyder, Nesheim, Wilkins, & Edmonds, 2013; Wilkins & Snyder, 2011) as

$$D_x^n = \frac{S^{7/10}}{R\tau_c^*} \left(\frac{Q_b n}{k_n B_b}\right)^{3/5}, \tag{11}$$

where R is the submerged specific gravity of sediment, τ_c^* is the dimensionless critical bed shear stress (or Shields parameter) for initiation of motion, and the subscript b on Q_b and B_b denotes that these values are at the specific flow condition when D_x is mobilized. Equation (11) is a rearranged and simplified form of the equation provided by Snyder et al. (2013). As discussed by Snyder et al. (2013), Equation (11) is expected to apply to gravel-bed rivers with low bedload sediment supply such that the local hydraulics, and not upstream sediment supply or other factors, control the bed sediment size distribution. To calculate D_x using Equation (11), only flow discharge that mobilizes D_x, with corresponding channel width, channel slope, and Manning's roughness must be known (R and τ_c^* are treated as constants). However, Manning's roughness can be written as a function of bed sediment grain size (Equation [9]), again assuming D_x is the percentile size of interest and that this percentile size contributes most to roughness. Therefore, upon substituting Equation (9) into Equation (11), D_x can be calculated as

$$D_x^- = \frac{\alpha_s^{1/9} S^{7/9}}{g^{1/3} \left(R\tau_c^*\right)^{10/9}} \left(\frac{Q_b}{ak_n B_b}\right)^{2/3}. \tag{12}$$

The superscript "−" denotes that this D_x (Equation 12) can be calculated with knowing only flow discharge that mobilizes D_x, corresponding channel width, and channel slope (g, k_n, α_s, a, R, and τ_c^* are treated as constants). This removes the dependence of the equation from Snyder et al. (2013) (Equation [11]) on Manning's roughness.

Finally, for calculating shear velocity we can remove the dependence of Equation (10) on a characteristic sediment size D_x by substituting in the D_x from Equation (12) and simplifying as

$$u_*^\tau = \left(\frac{\alpha_s}{R\tau_c^*}\right)^{1/18} \left(\frac{Q_b g}{ak_n B_b}\right)^{1/3} S^{7/18}. \tag{13}$$

The superscript τ denotes that this shear velocity was computed with a dimensionless critical bed shear stress (or Shields parameter) for initiation of motion of an implicit characteristic sediment size D_x at flow discharge Q_b. For Equation (13), shear velocity can be calculated with knowing only the flow discharge that mobilizes an implicit characteristic bed sediment percentile size, corresponding channel width, and channel slope (g, k_n, α_s, a, R, and τ_c^* are treated as constants). The assumptions/approximations inherent in Equation (13) include the following: (1) steady, uniform streamflow and (2) wide (width >> depth), rectangular channels; (3) most roughness is contributed by grain roughness from bed particles; (4) bedload sediment supply is low such that the local hydraulics control the bed sediment size distribution (5) there is an implicit characteristic sediment percentile tied to the specification of α_s; and (6) this sediment size is mobilized at the specified flow discharge with corresponding wetted channel width. Approximations (2) and (3) can be relaxed if appropriate modifications are made to the derivation. For near-threshold channels, the D_{50} sediment size is mobilized around bankfull flow (Parker, Wilcock, Paola,

Dietrich, & Pitlick, 2007; Phillips & Jerolmack, 2016), which typically corresponds to a 1.5- to 2-year recurrence interval flow (Leopold, Wolman, & Miller, 1964; Williams, 1978). If bankfull flow is used for Q_b, then bankfull width must be used for B_b. However, particularly for U.S. west-coast gravel-bed rivers, bed mobility can vary from this condition (Kaufmann, Faustini, Larsen, & Shirazi, 2008; Kaufmann, Larsen, & Faustini, 2009; Pfeiffer, Finnegan, & Willenbring, 2017). Equation (13) can still be used in this case as long as the mobility of the characteristic sediment size corresponds with the proper flow condition (perhaps not bankfull).

To summarize, we derived four equations for calculating shear velocity depending on what is known at a site (Table 1). The most field-intensive equation requires cross section surveys to calculate hydraulic radius R_h or average depth H (u_*^x, Equation [3]). In addition, this calculation requires knowing the channel slope S, which could also be surveyed in the field. The other equations (u_*^n, Equation [6]; u_*^D, Equation [10]; and u_*^τ, Equation [13]) require knowing at least flow discharge, channel width, and channel slope. In addition, Manning's roughness n must be known for u_*^n (Equation [6]) and a characteristic bed sediment grain size D_x must be known for u_*^D (Equation [10]). The established constants are $g = 9.81\,\mathrm{m/s^2}$, $k_n = 1$ if using SI units or 1.49 for English units, and $a = 8.1$ (García, 2008). The values of the parameters can vary, but typically $\alpha_s = 2$ when D_{50} is used for D_x (note that this value is tied to a specific D_x; see García, 2008), $R = 1.65$ for quartz but differs depending on minerology/lithology (Johnson & Olhoeft, 1984), and $\tau_c^* = 0.04$ for gravel-bed rivers (Snyder et al., 2013), although this value can vary from 0.03 to 0.07 (Buffington & Montgomery, 1997; Church, 2006; Lamb, Dietrich, & Venditti, 2008) and may require further adjustment depending if/how form roughness is accounted for (Buffington & Montgomery, 1997, 1999; Kaufmann et al., 2008; Lamb et al., 2008). The most uncertain of these parameters are α_s and τ_c^*. However, these are raised to the 1/18th power in Equation (13) compared to Q_b and B_b, which are raised to the 1/3rd power, and S, which is raised to the 7/18th power. Therefore, uncertainty in α_s and τ_c^* of say 10%, for the sake of argument, will alter the calculation of shear velocity by only 0.6% (Table 1). Also note that slope is raised to the largest exponent, so its importance in calculating shear velocity (and thus embeddedness) agrees with prior work highlighting the importance of channel slope in predicting fine sediment deposition on the bed (Naden et al., 2016; Relyea et al., 2012; Sutherland et al., 2010; Walters et al., 2003).

Key measures of aquatic benthic habitat are sediment grain size, embeddedness, and silt cover (we show later how shear velocity can predict embeddedness and silt cover). The equations derived above show how both sediment grain size (Equation [12]) and shear velocity (Equation [13]) can be estimated from flow discharge, channel width, and channel slope. The power and utility of these equations is that all three variables can be readily obtained from freely available, remotely sensed data in the United States. An approximation of bankfull discharge, as a 2-year recurrence interval flow, can be obtained for any river in the United States using regional regression equations as part of the U.S. Geological Survey's (USGS) StreamStats (USGS, 2021). Channel width can be obtained from georeferenced aerial photographs, which are available for the entire Earth from various sources at increasing spatial resolutions, or from lidar data, which are becoming more common as state-wide datasets. Channel slope can be calculated from digital elevation models (such as lidar) or for the United States, obtained directly from a channel segment in the National Hydrography Dataset (NHD; USEPA, 2021). Each of these datasets has associated errors that might currently limit the utility of applying Equation (13) everywhere. However, it is expected that these datasets will improve and become more accurate in time. This means that sediment grain size and shear velocity (and by extension, embeddedness) could be estimated remotely for many gravel-bed rivers in the entire United States for which the assumptions of the above equations apply.

The above equations are calculated for individual reaches. Equations (1)–(10) can be applied at any flow stage as long as the bed sediment is fully submerged. Equations (11)–(13) can only be applied at a specific flow discharge Q_b, typically the bankfull discharge, that mobilizes a characteristic sediment size, typically the D_{50}. Equation (13) could be reformulated to apply to any flow stage by keeping Q_b and B_b (from Equation [12]) separate from Q and B (from Equation [10]) when these two equations are combined. For this application, we focus on computing only bankfull shear velocity, as the channel forming condition, to build on the findings of Lamb and Venditti (2016).

TABLE 1 Summary of shear velocity equations, the inputs to each equation, and the sensitivity of u_* to a ± 10% change in each variable/parameter/constant

		Variables						Parameters			Constants		
		S	R_h	Q	B	n	D_x	α_s	R	τ_c^*	g	k_n	a
Equation		% change in u_* resulting from a ± 10% change of each input											
(3)	$u_*^x = \sqrt{gR_hS}$	5	5	–	–	–	–	–	–	–	5	–	–
(6)	$u_*^n = g^{1/2}\left(\frac{Qn}{k_nB}\right)^{3/10}S^{7/20}$	3.5	–	3	3	3	–	–	–	–	5	3	–
(10)	$u_*^D = (\alpha_sD_x)^{1/20}\left(\frac{Q}{ak_nB}\right)^{3/10}(gS)^{7/20}$	3.5	–	3	3	–	0.5	0.5	–	–	3.5	3	3
(13)	$u_*^\tau = \left(\frac{\alpha_s}{R\tau_c^*}\right)^{1/18}\left(\frac{Q_bg}{ak_nB_b}\right)^{1/3}S^{7/18}$	3.9	–	3.3	3.3	–	–	0.6	0.6	0.6	3.3	3.3	3.3

Note: Dashed entries indicate that the input is not included in an equation.

3 | STUDY AREA AND DATA COLLECTION

We measured channel geometry, embeddedness, and silt cover at 24 stream sites in the Piedmont region of Virginia and North Carolina during low flow in the summer of 2018 and six additional sites in the summer of 2019 (Figure 1). These sites span a range of conditions characteristic for the region, with drainage areas of 20–670 km^2, bankfull top widths of 8.5–34 m, and channel slopes of 0.001–0.02. The streams are gravel-bedded with a single channel containing riffles, pools, and runs. The upstream watersheds are on average 72% forested (range: 51%–90%), particularly on steep hillslopes, and with 15% pasture (range: 5%–32%; MRLC, 2016).

At each site, channel geometry was surveyed along three cross sections spaced roughly 1–2 channel widths apart using a Topcon GTS-105 Total Station. These data were georeferenced using a Trimble R10 real-time kinematic global positioning system. At each cross section, the bankfull elevation was determined as the lower of the two channel banks (Lindroth et al., 2020). At this bankfull elevation, we computed a bankfull hydraulic radius and averaged the three values together at each site.

We computed bankfull shear velocity in two ways by varying the equation used and the source of data. For both cases, we used values for the parameters and constants as defined above and channel slope from NHD (USEPA, 2021). The NHD slopes at four sites were 1–2 orders of magnitude lower than the others; for these sites, we replaced their slopes with values determined from the average bed elevations and streamwise distances between the three cross sections. The locations of some cross sections relative to pools and riffles for some sites (although not these four sites) precluded us from using these field estimates for all channel slopes because of concerns about the representativeness of these slopes for the reach. The two bankfull shear velocity estimates included the following: (1) u_*^x (Equation [3]) with the average bankfull hydraulic radius from our surveyed cross sections and (2) u_*^τ (Equation [13]) with bankfull flow approximated as the 2-year recurrence interval flow from USGS StreamStats (USGS, 2021) and average bankfull top width digitized from aerial photographs. The purpose of computing shear velocity in these two ways was to show what we believe to be our most accurate estimate, u_*^x, and that the results are similar when using freely available, remotely sensed data, u_*^τ.

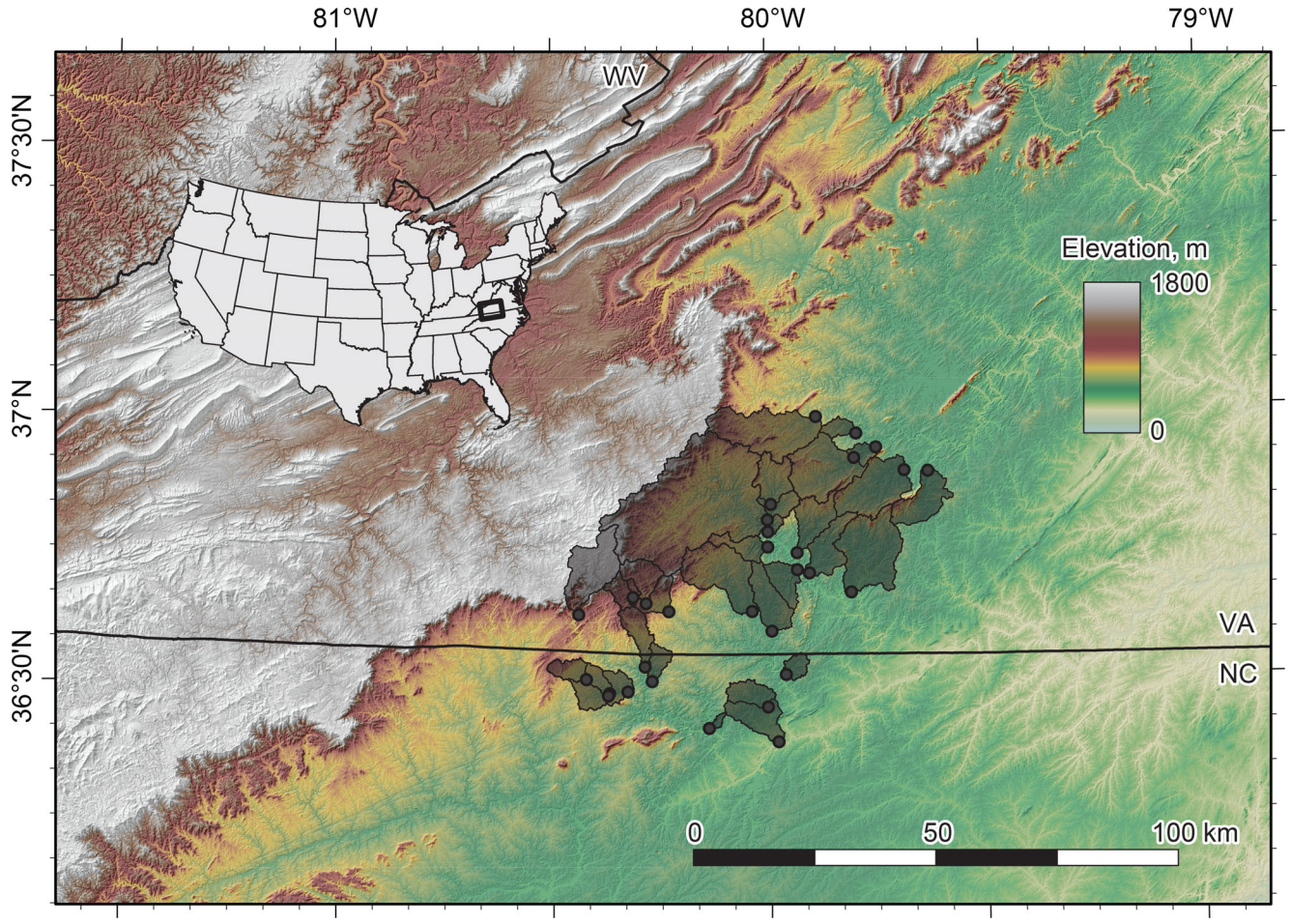

FIGURE 1 Study area map showing 30 sites and their watersheds in the Piedmont of Virginia and North Carolina. Symbols (circles) for two sites overlap at the resolution shown [Color figure can be viewed at wileyonlinelibrary.com]

For measuring embeddedness and silt cover, four to five cross-sectional transects reflecting riffle and run habitat were identified at each site to constitute a reach. Reach length was roughly 100–300 m and typically exceeded the cumulative span of the three surveyed cross sections. Along each transect, embeddedness and silt cover were measured within 0.6-m by 0.6-m quadrats spaced at 2-m intervals for streams >10 m wide or in five quadrats for streams <10 m wide. Embeddedness was visually estimated as the percentage (to the nearest 20%) of the surface area of the gravel or coarser substrate covered by sand or finer sediment (<2 mm; based on Fitzpatrick et al., 1998; akin to Platts, Megahan, & Minshall, 1983). In addition, the height of embeddedness for five particles in each quadrat (middle and four corners) was measured (Fitzpatrick et al., 1998), averaged together, and compared to the visual estimates of embeddedness. The two measures of embeddedness were highly correlated (>0.95), so we only used the visual estimates of embeddedness moving forward. Silt cover was visually estimated as the percentage (to the nearest 20%) of the surface area of the gravel or coarser substrate with an accumulation of very fine, inorganic or organic, particulates (<62.5 μm; e.g., Dunn & Angermeier, 2016). We calculated median embeddedness and silt cover across all quadrats at a transect and then calculated median reach-level embeddedness and silt cover across the four to five median transect-level embeddedness and silt cover values at each reach (site). Of the 24 sites measured in 2018, 22 were measured twice (during low flow in early and late summer) in 2018 and twice in 2019 for a total of four measurements of median reach-level embeddedness and silt cover. We did not attempt to replicate the exact locations of quadrats during repeat samples. One site was measured only once in 2018 but twice in 2019, and one site was measured twice in 2018 but not in 2019. The six sites measured for the first time in 2019 were measured twice. From these two to four measurements of median reach-level embeddedness and silt cover at each site, we computed the mean, maximum, and minimum values for each site.

4 | RESULTS

Our data are consistent with our hypothesis. Near the critical value of bankfull shear velocity (0.1 m/s), embeddedness approaches 100% and as bankfull shear velocity increases, embeddedness gradually decreases (Figure 2). This result is novel because it shows that a baseline level of embeddedness can be predicted independently of sediment supply.

There is one major outlier (marked with a red star in Figure 2) that has a high value of embeddedness compared to other values at a similar shear velocity. This site is along Big Beaver Island Creek in Madison, NC, where we observed bank erosion during a high flow event and bank migration upon subsequent field visits. Therefore, at locations with high sediment supply, actual embeddedness is expected to be greater than the predicted baseline level.

We obtain the following best-fit power-law relations for our two values of bankfull shear velocity, including all measurements:

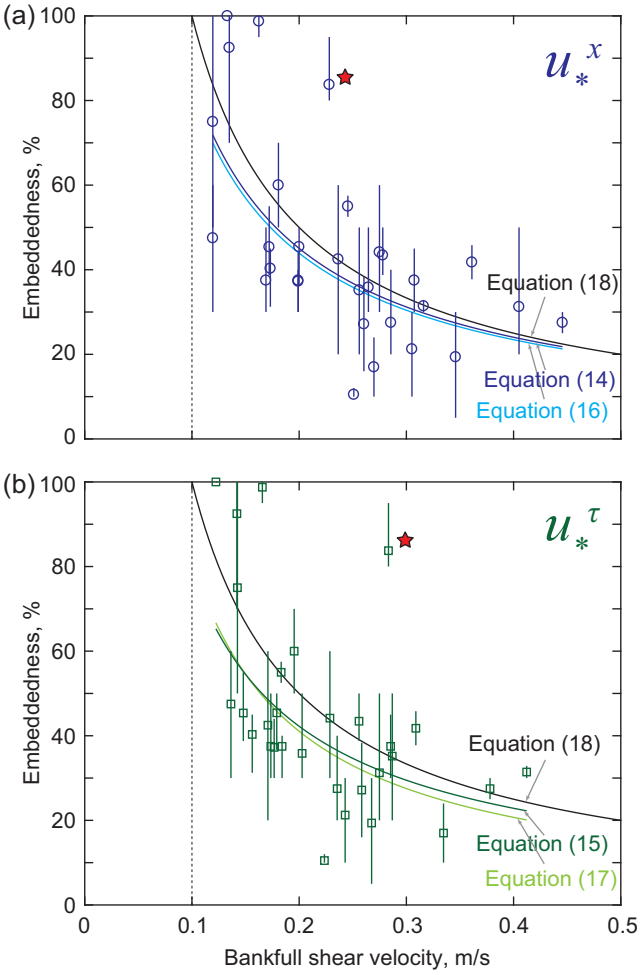

FIGURE 2 A baseline level of embeddedness is predictable from bankfull shear velocity when bankfull shear velocity exceeds the critical value of 0.1 m/s. Plotted power-law curves show predicted values of embeddedness as a percentage, E_p, versus bankfull shear velocity calculated as (a) u_*^x and (b) u_*^τ. Each point is the mean embeddedness at a site and the vertical lines on each point extend to the maximum and minimum measurements of embeddedness. The red star indicates the site known to have a high sediment supply (see text for discussion) [Color figure can be viewed at wileyonlinelibrary.com]

$$E_p = 10.5\left(u_*^x\right)^{-0.91}\left(R^2 = 0.38, p = .0003, n = 30\right), \quad (14)$$

$$E_p = 10.1\left(u_*^\tau\right)^{-0.89}\left(R^2 = 0.30, p = .0018, n = 30\right), \quad (15)$$

or excluding the one outlier:

$$E_p = 10.2\left(u_*^x\right)^{-0.90}\left(R^2 = 0.41, p = .0002, n = 29\right), \quad (16)$$

$$E_p = 8.4\left(u_*^\tau\right)^{-0.99}\left(R^2 = 0.39, p = .0003, n = 29\right), \quad (17)$$

where E_p is embeddedness as a percentage and u_*^x and u_*^τ are our two calculated values of bankfull shear velocity in m/s. These equations roughly generalize to

$$E_p = \frac{10}{u_*}, \tag{18}$$

or

$$E_f = \frac{1}{10u_*}, \tag{19}$$

where E_f is embeddedness as a fraction and u_* is the bankfull shear velocity in m/s. Thus, in general (Equation [18]), embeddedness is inversely proportional to shear velocity (for values >0.1 m/s). Roughly, from Equation (18), a bankfull shear velocity of 0.1 m/s corresponds to 100% embeddedness, a bankfull shear velocity of 0.2 m/s corresponds to 50% embeddedness, and a bankfull shear velocity of 0.5 m/s corresponds to 20% embeddedness (black line, Figure 2). Furthermore, from our data, for u_* < ~0.25 m/s, embeddedness is almost always above 40% and for u_* > ~0.25 m/s, embeddedness is almost always below 40% (Figure 2).

Similarly, our data also show that silt cover decreases with increasing bankfull shear velocity (>0.1 m/s; Figure 3). We obtain the following best-fit power-law relations for our two values of bankfull shear velocity:

$$SC_p = 8.4\left(u_*^x\right)^{-0.61}\left(R^2 = 0.17, p = .025, n = 30\right), \tag{20}$$

$$SC_p = 8.2\left(u_*^\tau\right)^{-0.59}\left(R^2 = 0.13, p = .049, n = 30\right), \tag{21}$$

where SC_p is silt cover as a percentage. These equations roughly generalize to

$$SC_p = \frac{10}{\sqrt{u_*}}, \tag{22}$$

or

$$SC_f = \frac{1}{10\sqrt{u_*}}, \tag{23}$$

where SC_f is silt cover as a fraction. Thus, in general (Equation [22]), silt cover is also inversely proportional to bankfull shear velocity (for values >0.1 m/s), although silt cover is less precisely predictable from bankfull shear velocity than embeddedness (see also Scott & Villamagna, 2020). Perhaps most importantly for silt cover, the generalized Equation (18) for embeddedness appears to constrain the maximum measured value of silt cover as

$$SC_{p,\max} = \frac{10}{u_*}, \tag{24}$$

or

$$SC_{f,\max} = \frac{1}{10u_*}, \tag{25}$$

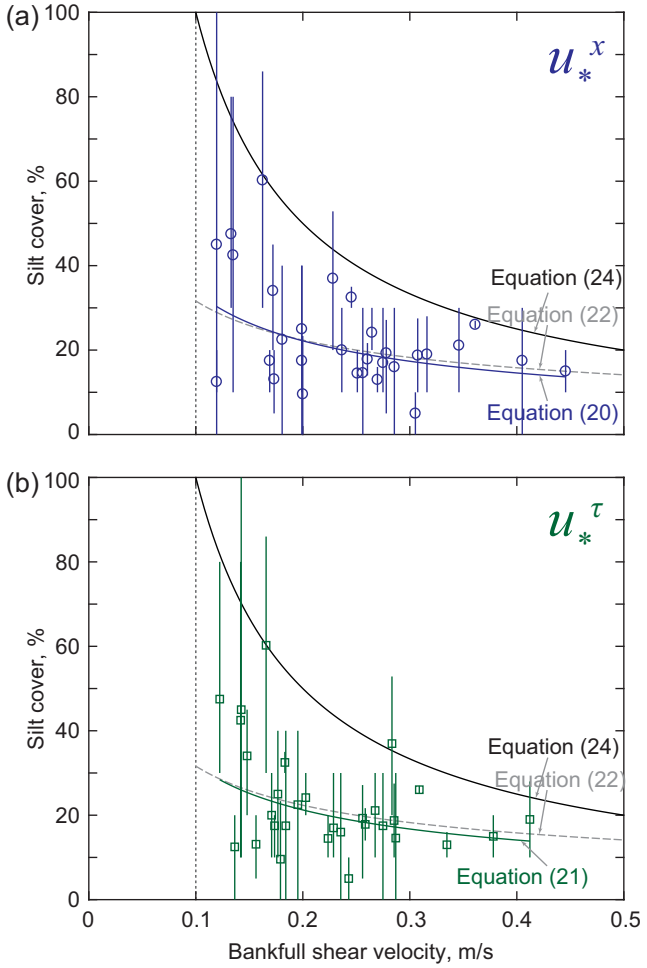

FIGURE 3 The maximum value of silt cover is predictable from bankfull shear velocity when bankfull shear velocity exceeds the critical value of 0.1 m/s. Plotted power-law curves show predicted values of silt cover as a percentage, SC_p, versus bankfull shear velocity calculated as (a) u_*^x and (b) u_*^τ. Each point is the mean silt cover at a site, and the vertical lines on each point extend to the maximum and minimum measurements of silt cover [Color figure can be viewed at wileyonlinelibrary.com]

where $SC_{p,\max}$ is the maximum silt cover as a percentage and $SC_{f,\max}$ is the maximum silt cover as a fraction.

5 | DISCUSSION AND CONCLUSION

Shear velocity is related to turbulence keeping particles in suspension (García, 2008; Niño et al., 2003). Therefore, from a process-based perspective, shear velocity should help predict fine sediment deposition on gravel streambeds. Embeddedness is more predictable than silt cover, and we suspect that the simple generalized form (Equation [18]) describing the gradual decrease in these values as bankfull shear velocity increases may be possible to theoretically derive. We suggest that bankfull shear velocity determines how much fine sediment is transported near the bed or in suspension when the

gravel bed is fully mobilized and, once the flow decreases and gravel transport ceases, the near-bed fine sediment becomes the fine matrix of the gravel bed (establishing a baseline value of embeddedness). This is consistent with Lisle (1989), who found that most infiltrated sediment originated from the finest fraction of the bedload rather than from settled suspended load. The amount of fine sediment in the pore spaces of the gravel bed can fluctuate in time (via winnowing or further deposition; see review in Wharton et al., 2017), but would return to its baseline value once the gravel bed is remobilized at each flow above bankfull. Some of the observed variance in embeddedness not explained by bankfull shear velocity may be related to unknown amounts of infiltration and winnowing that could have occurred after the spring high flows that likely mobilized the bed but before the summer low-flow measurements.

We suspect that our embeddedness predictions are representative of a baseline gravel-bed state under low sediment supply conditions. This method could be used to identify locations with strongly altered sediment supply (Figure 4a). For augmented sediment supply beyond what would be controlled by streamflow hydraulics, these points would plot toward the top right of Figure 4a (also see outlier in Figure 2). For greatly reduced sediment supply where more winnowing is occurring, these points would plot toward the bottom left of Figure 4a.

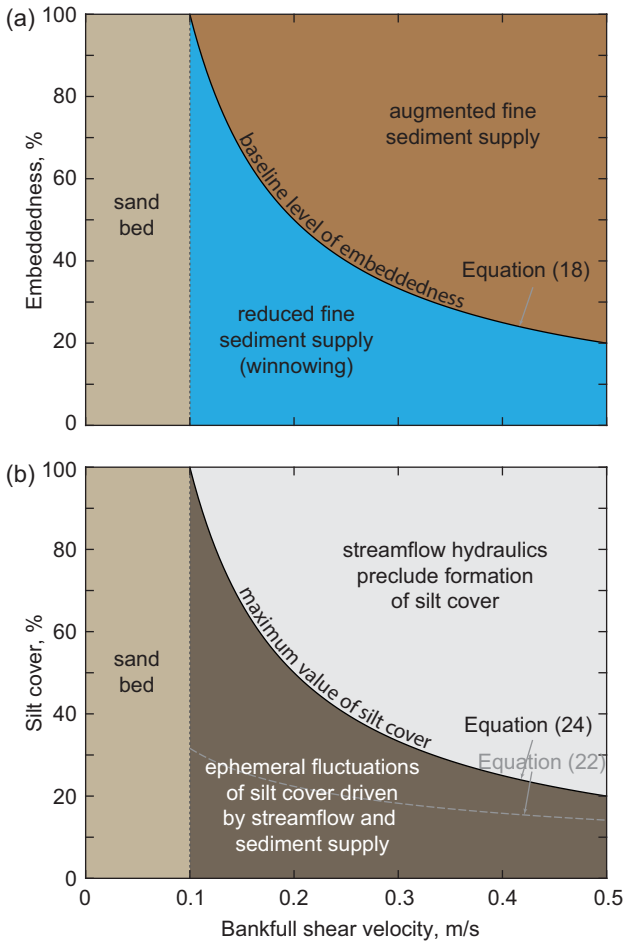

FIGURE 4 Conceptual overview of how bankfull shear velocity in gravel-bed rivers (right side of panels) affects percentages of (a) embeddedness and (b) silt cover [Color figure can be viewed at wileyonlinelibrary.com]

Silt cover is ephemeral, often forming a temporary mud drape on the streambed during receding or low-flow conditions, and is easily mobilized by the next moderate/high flow (Carling & Reader, 1982; Droppo & Stone, 1994; Wood & Armitage, 1997). Therefore, silt cover is expected to fluctuate greatly at a site and other factors, such as sediment supply and flood frequency, may drive variation in silt cover (Figure 4b). The maximum value of silt cover is likely controlled by streamflow hydraulics, which is why it appears to be most predictably constrained (Figures 3 and 4b). Furthermore, because embeddedness appears to constrain the maximum value of silt cover, the supply of silt for draping the streambed may come from the sediments embedding the larger particles.

Both methods of estimating bankfull shear velocity (Equation [3] and [13]) result in similar values (see Figures 2 and 3). Thus, for this study area, estimating bankfull shear velocity using Equation (13) and freely available, remotely sensed data is a reasonable approach. Further analysis of existing datasets is needed to test the utility of bankfull shear velocity for predicting embeddedness in regions outside the Piedmont of the Mid-Atlantic region, particularly those with much larger sediment supply (e.g., the Pacific Northwest, Kaufmann et al., 2008, 2009). We caution future researchers to work with the most accurate channel slope data available and to consider whether additional modifications to the equations are necessary to account for form roughness to obtain the most accurate estimates of shear velocity.

Our work demonstrates how bankfull shear velocity can be estimated in the United States from freely available, remotely sensed data of bankfull discharge, channel width, and channel slope. Such estimates can predict a baseline level of embeddedness and a maximum value of silt cover at a reach scale independently of knowing sediment supply. In addition, this theoretical foundation moves us one step closer to developing predictive statistical models that link geophysical processes in streams with biotic responses mediated by benthic habitat metrics such as embeddedness and silt cover. Ultimately, further application and extension of our work may provide insight for aquatic ecosystem managers and researchers into how river network structure and processes influence the spatial distribution of habitats and biotic assemblages.

ACKNOWLEDGMENTS

This work was partially supported by the National Fish and Wildlife Foundation (8020.18.059147), Virginia Agricultural Experiment Station, and USDA Hatch program (1017457). The Virginia Cooperative Fish and Wildlife Research Unit is jointly sponsored by the U.S. Geological Survey, Virginia Tech, Virginia Department of Wildlife Resources, and Wildlife Management Institute. Any use of trade, firm, or product names is for descriptive purposes only and does not imply endorsement by the U.S. Government. We thank Rebecca Hodge (Durham University), Robb Jacobson (USGS), and an anonymous

reviewer for their comments that helped improve the presentation of our work and the Editor (Martin Thoms) for handling our manuscript.

CONFLICT OF INTEREST

The authors have no conflict of interest to declare.

DATA AVAILABILITY STATEMENT

Datasets for this research are available through HydroShare: https://doi.org/10.4211/hs.57753ddbdf6545f689d70c9d01b7965a.

ORCID

Jonathan A. Czuba https://orcid.org/0000-0002-9485-2604

REFERENCES

Brunke, M. (1999). Colmation and depth filtration within streambeds: Retention of particles in hyporheic interstices. *International Review of Hydrobiology*, *84*(2), 99–117. https://doi.org/10.1002/iroh.199900014

Buffington, J. M., & Montgomery, D. R. (1997). A systematic analysis of eight decades of incipient motion studies, with special reference to gravel-bedded rivers. *Water Resources Research*, *33*(8), 1993–2039. https://doi.org/10.1029/96WR03190

Buffington, J. M., & Montgomery, D. R. (1999). Effects of hydraulic roughness on surface textures of gravel-bed rivers. *Water Resources Research*, *35*(11), 3507–3521. https://doi.org/10.1029/1999WR900138

Carling, P. A., & Reader, N. A. (1982). Structure, composition and bulk properties of upland stream gravels. *Earth Surface Processes and Landforms*, *7*(4), 349–365. https://doi.org/10.1002/esp.3290070407

Church, M. (2006). Bed material transport and the morphology of alluvial river channels. *Annual Review of Earth and Planetary Sciences*, *34*, 325–354. https://doi.org/10.1146/annurev.earth.33.092203.122721

Cowan, W. L. (1956). Estimating hydraulic roughness coefficients. *Agricultural Engineering*, *337*, 470–500.

Droppo, I. G., & Stone, M. (1994). In-channel surficial fine-grained sediment laminae. Part I: Physical characteristics and formational processes. *Hydrological Processes*, *8*(2), 101–111. https://doi.org/10.1002/hyp.3360080202

Dunn, C. G., & Angermeier, P. L. (2016). Development of habitat suitability indices for the candy darter, with cross-scale validation across representative populations. *Transactions of the American Fisheries Society*, *145*(6), 1266–1281. https://doi.org/10.1080/00028487.2016.1217929

Fitzpatrick, F. A., Waite, I. R., D'Arconte, P. J., Meador, M. R., Maupin, M. A., & Gurtz, M. E. (1998). Revised methods for characterizing stream habitat in the National Water-Quality Assessment Program. USGS WRI report 98-4052. Retrieved from https://pubs.usgs.gov/wri/wri984052/pdf/wri98-4052.pdf

García, M. H. (2008). Sediment transport and morphodynamics. In M. H. García (Ed.), *Sedimentation engineering: Processes, measurements, modeling, and practice: ASCE manuals and reports on engineering practice*, *110* (pp. 21–163). Reston, VA: ASCE.

Johnson, G. R., & Olhoeft, G. R. (1984). Density of rocks and minerals. In R. S. Carmichael (Ed.), *CRC handbook of physical properties of rocks: Volume III* (1st ed., pp. 1–38). Boca Raton, FL: CRC Press. https://doi.org/10.1201/9780203712030

Kaufmann, P. R., Faustini, J. M., Larsen, D. P., & Shirazi, M. A. (2008). A roughness-corrected index of relative bed stability for regional stream surveys. *Geomorphology*, *99*(1–4), 150–170. https://doi.org/10.1016/j.geomorph.2007.10.007

Kaufmann, P. R., Larsen, D. P., & Faustini, J. M. (2009). Bed stability and sedimentation associated with human disturbances in Pacific northwest streams. *Journal of the American Water Resources Association*, *45*(2), 434–459. https://doi.org/10.1111/j.1752-1688.2009.00301.x

Kemp, P., Sear, D., Collins, A., Naden, P., & Jones, I. (2011). The impacts of fine sediment on riverine fish. *Hydrological Processes*, *25*(11), 1800–1821. https://doi.org/10.1002/hyp.7940

Lamb, M. P., Brun, F., & Fuller, B. M. (2017). Direct measurements of lift and drag on shallowly submerged cobbles in steep streams: Implications for flow resistance and sediment transport. *Water Resources Research*, *53*(9), 7607–7629. https://doi.org/10.1002/2017WR020883

Lamb, M. P., Dietrich, W. E., & Venditti, J. G. (2008). Is the critical shields stress for incipient sediment motion dependent on channel-bed slope? *Journal of Geophysical Research - Earth Surface*, *113*(F2), F02008. https://doi.org/10.1029/2007JF000831

Lamb, M. P., & Venditti, J. G. (2016). The grain size gap and abrupt gravel-sand transitions in rivers due to suspension fallout. *Geophysical Research Letters*, *43*, 3777–3785. https://doi.org/10.1002/2016GL068713

Leopold, L. B., Wolman, M. G., & Miller, J. P. (1964). *Fluvial processes in geomorphology* (p. 522). San Francisco, CA: W. H. Freeman and Company.

Lindroth, E. M., Rhoads, B. L., Castillo, C. R., Czuba, J. A., Güneralp, İ., & Edmonds, D. (2020). Spatial variability in bankfull stage and bank elevations of lowland meandering rivers: Relation to rating curves and channel planform characteristics. *Water Resources Research*, *56*(8), e2020WR027477. https://doi.org/10.1029/2020WR027477

Lisle, T. E. (1989). Sediment transport and resulting deposition in spawning gravels, north coastal California. *Water Resources Research*, *25*(6), 1303–1319. https://doi.org/10.1029/WR025i006p01303

Multi-Resolution Land Characteristics Consortium (MRLC). (2016). National Land Cover Database 2016. Retrieved from https://www.mrlc.gov/data/nlcd-2016-land-cover-conus

Naden, P. S., Murphy, J. F., Old, G. H., Newman, J., Scarlett, P., Harman, M., … Jones, J. I. (2016). Understanding the controls on deposited fine sediment in the streams of agricultural catchments. *Science of the Total Environment*, *547*, 366–381. https://doi.org/10.1016/j.scitotenv.2015.12.079

Niño, Y., Lopez, F., & García, M. (2003). Threshold for particle entrainment into suspension. *Sedimentology*, *50*(2), 247–263. https://doi.org/10.1046/j.1365-3091.2003.00551.x

Parker, G., Wilcock, P. R., Paola, C., Dietrich, W. E., & Pitlick, J. (2007). Physical basis for quasi-universal relations describing bankfull hydraulic geometry of single-thread gravel bed rivers. *Journal of Geophysical Research - Earth Surface*, *112*(F4), F04005. https://doi.org/10.1029/2006JF000549

Pfeiffer, A. M., Finnegan, N. J., & Willenbring, J. K. (2017). Sediment supply controls equilibrium channel geometry in gravel rivers. *Proceedings of the National Academy of Sciences of the United States of America*, *114*(13), 3346–3351. https://doi.org/10.1073/pnas.1612907114

Phillips, C. B., & Jerolmack, D. J. (2016). Self-organization of river channels as a critical filter on climate signals. *Science*, *352*(6286), 694–697. https://doi.org/10.1126/science.aad3348

Platts, W. S., Megahan, W. F., & Minshall, W. G. (1983). Methods for evaluating stream, riparian, and biotic conditions. General Technical Report INT-138, USDA Forest Service, Rocky Mountain Research Station. Ogden, UT. p. 76.

Relyea, C. D., Minshall, G. W., & Danehy, R. J. (2012). Development and validation of an aquatic fine sediment biotic index. *Environmental Management*, *49*, 242–252. https://doi.org/10.1007/s00267-011-9784-3

Rickenmann, D., & Recking, A. (2011). Evaluation of flow resistance in gravel-bed rivers through a large field data set. *Water Resources Research*, *47*(7), W07538. https://doi.org/10.1029/2010WR009793

Scott, L., & Villamagna, A. (2020). SWAT vs. RUSLE: Which better predicts benthic habitat condition? *Journal of Soil and Water Conservation*, *75*, 765–774. https://doi.org/10.2489/jswc.2020.00183

Sennatt, K. M., Salant, N. L., Renshaw, C. E., & Magilligan, F. J. (2006). Assessment of methods for measuring embeddedness: Application to sedimentation in flow regulated streams. *Journal of the American Water*

Resources Association, *42*(6), 1671–1682. https://doi.org/10.1111/j.1752-1688.2006.tb06028.x

Snyder, N. P., Nesheim, A. O., Wilkins, B. C., & Edmonds, D. A. (2013). Predicting grain size in gravel-bedded rivers using digital elevation models: Application to three Maine watersheds. *GSA Bulletin*, *125*(1–2), 148–163. https://doi.org/10.1130/B30694.1

Sutherland, A. B., Culp, J. M., & Benoy, G. A. (2010). Characterizing deposited sediment for stream habitat assessment. *Limnology and Oceanography: Methods*, *8*(1), 30–44. https://doi.org/10.4319/lom.2010.8.30

USEPA, U.S. Environmental Protection Agency. (2020). National summary of impaired waters and TMDL information. Retrieved June 12, 2020 from https://ofmpub.epa.gov/tmdl_waters10/attains_nation_cy.control?p_report_type=T

USEPA, U.S. Environmental Protection Agency. (2021). National Hydrography Dataset (NHDPlusV2). Retrieved February 15, 2021 from https://www.epa.gov/waterdata/get-nhdplus-national-hydrography-dataset-plus-data

USGS, U.S. Geological Survey. (2021). StreamStats Retrieved February 15, 2021 from https://streamstats.usgs.gov/ss/

Walters, D. M., Leigh, D. S., Freeman, M. C., Freeman, B. J., & Pringle, C. M. (2003). Geomorphology and fish assemblages in a Piedmont river basin, U.S.A. *Freshwater Biology*, *48*(11), 1950–1970. https://doi.org/10.1046/j.1365-2427.2003.01137.x

Wharton, G., Mohajeri, S. H., & Righetti, M. (2017). The pernicious problem of streambed colmation: A multi-disciplinary reflection on the mechanisms, causes, impacts, and management challenges. *WIREs Water*, *4*, e1231. https://doi.org/10.1002/wat2.1231

Wilkins, B. C., & Snyder, N. P. (2011). Geomorphic comparison of two Atlantic coastal rivers: Toward an understanding of physical controls on Atlantic salmon habitat. *River Research and Applications*, *27*(2), 135–156. https://doi.org/10.1002/rra.1343

Williams, G. P. (1978). Bank-full discharge of rivers. *Water Resources Research*, *14*(6), 1141–1154. https://doi.org/10.1029/WR014i006p01141

Wood, P. J., & Armitage, P. D. (1997). Biological effects of fine sediment in the lotic environment. *Environmental Management*, *21*, 203–217. https://doi.org/10.1007/s002679900019

Yochum, S. E., Bledsoe, B. P., David, G. C. L., & Wohl, E. (2012). Velocity prediction in high-gradient channels. *Journal of Hydrology*, *424-425*, 84–98. https://doi.org/10.1016/j.jhydrol.2011.12.031

How to cite this article: Czuba, J. A., Hirschler, M., Pratt, E. A., Villamagna, A., & Angermeier, P. L. (2022). Bankfull shear velocity predicts embeddedness and silt cover in gravel streambeds. *River Research and Applications*, *38*(1), 59–68. https://doi.org/10.1002/rra.3878